

# Passive Shock-Wave/Boundary-Layer Control on a Wall-Mounted Model

S. Raghunathan\*

*The Queen's University of Belfast, Belfast, Northern Ireland*  
and

D. G. Mabey†

*Royal Aircraft Establishment, Bedford, England*

Tests were made on a roof-mounted 6%-thick part section circular arc model in a small transonic tunnel at transonic Mach numbers to evaluate the effects of the orientation of holes on the passive shock-wave/boundary-layer control. Three hole orientations were investigated; normal, forward-facing and backward-facing. The porosity was 1.6%. The measurements included static and dynamic pressures on the model's surface, wake traverses, and shadowgraphs. The forward-facing holes located around the shock position show an appreciable decrease in drag when compared with a solid surface model.

## Nomenclature

$C_D$	= profile drag coefficient
$C_p$	= pressure coefficient
$c$	= model chord length
$f$	= frequency
$h$	= phenum depth
$\sqrt{nF(n)}$	= forcing function
$M_{S0}$	= Mach number, shock Mach number at zero porosity
$n$	= frequency parameter $fc/u$
$p$	= porosity open area/model area
$\bar{p}$	= rms value of pressure fluctuations
$p_{0,\infty}$	= stagnation pressure, freestream
$q_\infty$	= freestream dynamic pressure
$U_\infty$	= freestream velocity
$X_{p,S}$	= distance along the chord, porous region, shock position
$y$	= distance normal to the chord

## Introduction

A METHOD adopted in recent years to reduce the drag associated with shock waves and improve performance envelopes for transonic aircraft is the use of supercritical shock-free airfoil sections for the wings. But this method is effective only at the design flight condition. The drag increases rapidly at off-design conditions, particularly for thick airfoil sections.

A simple and economical concept for drag reduction at transonic speeds appears to be the passive shock wave/boundary-layer control. The concept consists of having a porous surface with a plenum chamber under the shock location. The high pressure downstream of the shock wave forces some of the boundary-layer flow into the plenum and out ahead of the shock wave. The boundary layer ahead of the shock wave is thickened, and compression waves are formed in the supersonic region, thereby reducing the entropy change and pressure gradient and flow separation.

Investigation<sup>1-3</sup> in the United States with a wall-mounted 12%-thick circular arc half-model and a 12%-thick supercritical airfoil in a 3-in.  $\times$  12.4-in. transonic tunnel have shown that a reduction in drag can be achieved with a 2.5% porosity in the region of shock-wave/boundary-layer interaction. These experiments were restricted to models with normal holes and at a constant porosity distribution in the region of shock wave and did not include any unsteady flow measurements.

The passive effect of a porous surface in the shock-wave/boundary-layer interaction was observed by Krogmann et al.<sup>4</sup> Their experiments in the 1-m  $\times$  1-m transonic wind tunnel at Göttingen on a supercritical airfoil showed that whereas the passive effect is predominant at relatively high shock Mach numbers for a perforated surface, its favorable effect is present over a wide range of Mach numbers for a slotted surface. For a double-slotted configuration, at high angles of attack no severe buffeting was noticed even though the flow was separated near the trailing edge.

In the experiments of Krogmann et al., the control appears to be at the foot of the shock or possible downstream of the shock for the double slot and perforated surfaces. The experiments were not made at constant porosity, and it is therefore difficult to compare the results of the slotted models with those of porous models.

Further, if the ratio of the boundary-layer thickness to the diameter of the holes or width of a slot is important, then this could explain some of the differences among the three cases.

A theoretical analysis by Savu et al.<sup>5</sup> and Chen et al.<sup>6</sup> suggest that a varying porosity produces a larger drag reduction than a constant porosity and, further, that the lift actually increases on a porous model when compared with a solid model.

In order to gain further physical understanding of transonic shock/boundary-layer interaction with a passive boundary-layer control, a program of research was undertaken in a 10-cm  $\times$  10-cm transonic tunnel with a roof-mounted 6% thick circular arc model. The first phase of this investigation is reported here.

## Test Facility and Models

Experiments were made in a blowdown transonic wind tunnel with an atmospheric intake. The test section (Fig. 1) had closed sidewalls and a slotted floor with two slots covered with screens. The porosity of the floor was 9.6%.

The model was a circular arc half-airfoil 101.6 mm chord, 6% thick, set on the closed tunnel roof at a distance of 610 mm from the leading edge of the slots on the floor of the tunnel (Fig. 2).

Received Oct. 30, 1985; presented as Paper 86-0285 at the AIAA 24th Aerospace Sciences Meeting, Reno, NV, Jan. 6-9, 1986; revision received June 6, 1986. Copyright © American Institute of Aeronautics and Astronautics, Inc., 1986. All rights reserved.

\*Senior Lecturer, Department of Aeronautical Engineering, Member AIAA.

†Principal Scientific Officer, Dynamics Laboratory.

Earlier experiments have shown that the momentum thickness Reynolds  $R_\theta$  at the foot of the shock of  $10^4$  can be obtained at this model position.

Four models were tested. Three of them has porous surfaces with a plenum chamber underneath in the region extending from 53% to 93% of the chord length and spanning 87% of the model span. The porous surfaces were obtained by drilling 1-mm-diam holes normal to the surface (NH), inclined at 60 deg to the normal to the surface and forward-facing (FFH), and inclined at 60 deg to the normal and backward-facing (BFH). The ratio of the hole diameter to the displacement thickness of the boundary layer at the foot of the shock was about 1. The porosity on the model (based on the area of the holes to the total area of the model) was variable from zero to 3.16%. The plenum chamber beneath the porous surface had an average depth of  $h=4$  mm, corresponding to a ratio of boundary-layer displacement thickness upstream of the shock wave to plenum depth of  $\delta^*/h=0.25$ . The fourth model was a solid model with zero porosity. All the models had pressure orifices located at 5-mm intervals up to the midchord position and 2.5-mm intervals between the midchord and trailing edge.

Three shock Mach numbers of  $M_{S0}$  1.2, 1.3, and 1.37 with reference to the solid model (SM) were chosen for experiments. The corresponding shock positions were  $X_{S0}/C = 0.70, 0.80$ , and  $0.85$ . This compares with the experiments done by Mabey et al.<sup>7</sup> periodic flows on a slightly thicker biconvex airfoil (14% thick), where the shock Mach numbers and shock positions were within the range  $M_S = 1.2$ –1.3 and  $X_S/C = 0.60$ –0.65. For all the experiments with porosity, the porous region  $X_P/C$  was kept the same, from  $0.75 X/C$  to  $0.88 X/C$ .

A Scanivalve with a pressure storage box was used for pressure measurements. Wake traverses were performed at a position  $x/c = 1.1$  on the center line of the model. A pitot tube with a front opening of  $0.7 \text{ mm} \times 2 \text{ mm}$  and a Druck PDCR 32 transducer was used for this purpose. For some of the test, shadowgraph pictures with an exposure time of 0.1 s were taken. Other measurements included some unsteady pressure measurements at a selected location of 93% chord for the zero porosity and FFH model with Kulite transducer.

The freestream Mach numbers were based on a sidewall pressure tapping two chords upstreams of the model leading edge. The freestream Mach number in the tunnel was varied by a choke downstream of the test section.

It should be noted that all the experiments were conducted at a tunnel-height/model-chord ratio of 1, and therefore the interference between the supersonic bubble and the tunnel floor could be significant enough to affect the overall results. This, however, does not invalidate the comparison between the results of solid model and porous models.

## Results and Discussions

The pressure distributions for all the three porous models compared with the SM model for  $M_{S0} = 1.2, 1.3$ , and  $1.37$  are shown in Figs. 3, 4, and 5, respectively. The porosity for the three porous models NH, FFH, and BFH is 0.016.

The results shown in Fig. 3, where the shock position is upstream of the porous surfaces, is very relevant to aircraft wings. If the concept of the passive shock-wave/boundary-layer control is used on a supercritical wing, the region of porosity is to be downstream of the shock wave at the design conditions so that at a higher flight Mach number, the shock becomes stronger and moves downstream, bringing the passive control into operation. It can be observed from Fig. 3 that the porosity downstream of the shock wave does affect the pressure distribution downstream of the shock wave. There appears to be a separated or recirculating flow in the porous region when the results of porous models are compared with the solid model. Either flow separation or recirculation can change the effective surface profile and therefore the pressure distribution. There are also small changes in the shock positions of the porous models when compared with the

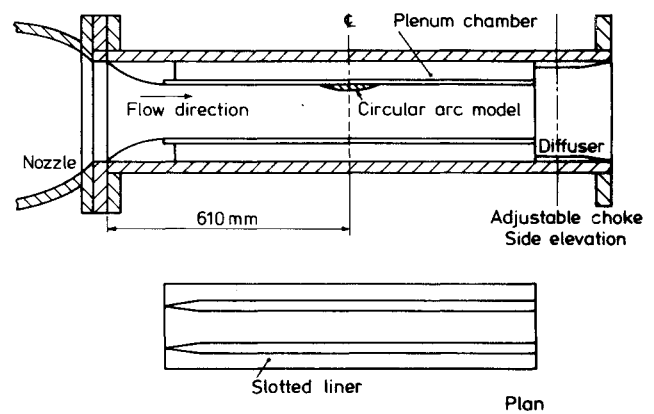


Fig. 1 The test section.

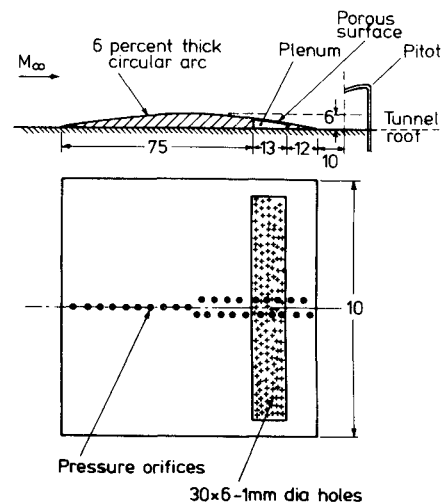


Fig. 2 The model.

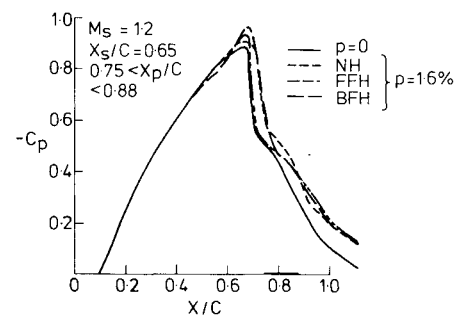


Fig. 3 Pressure distribution on the model,  $M_{S0} = 1.2$ .

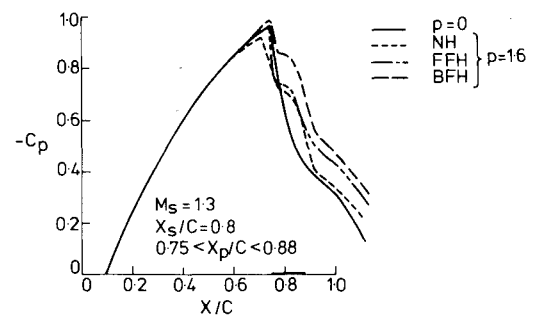
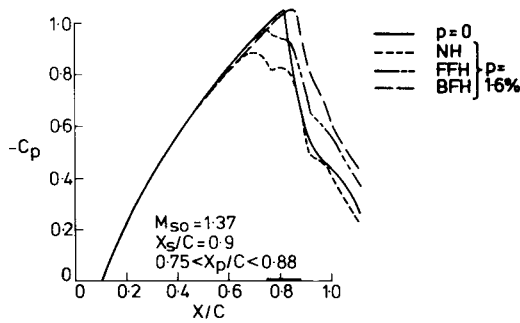
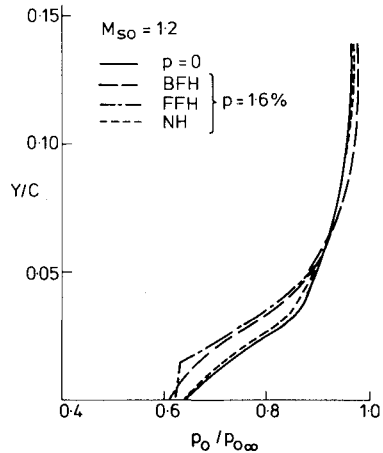
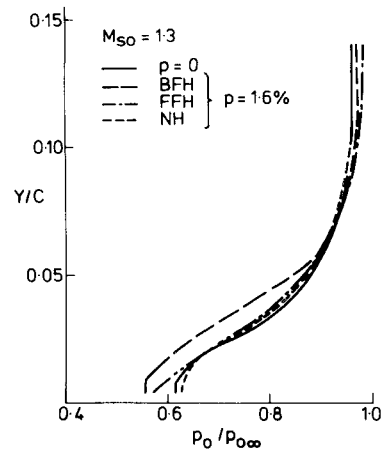


Fig. 4 Pressure distribution on the model,  $M_{S0} = 1.3$ .

Fig. 5 Pressure distribution on the model,  $M_{S0} = 1.37$ .Fig. 9 Total pressure profiles in the wake,  $M_{S0} = 1.2$ .Fig. 6 Shadowgraphs,  $M_{S0} = 1.2$ .Fig. 7 Shadowgraphs,  $M_{S0} = 1.3$ .Fig. 8 Shadowgraphs,  $M_{S0} = 1.37$ .

SM model (this can also be observed from the diagrams based on the shadowgraphs corresponding to this test condition shown in Fig. 6). It is observed that for the NH model there is a second shock wave close to the leading edge of the porous region where a significant departure in the pressure distribution occurs, indicating that there is an airflow from the plenum changing the effective shape of the airfoil. The existence of the airflow in and out of the plenum can also be deduced from the appreciable changes in the values of  $C_p$  at the trailing edge for all the porous model. Generally, the trailing edge  $C_p$  for a porous model is lower than that for a solid model.

Figure 4 corresponds to the shock-wave position just at the beginning of the porous surface. The corresponding shadowgraphs are shown in Fig. 7. The differences in pressure distributions for the four models are considerable when compared with the SM model. Normal holes produce a slight movement of the shock forward. The FFH and BFH do not produce appreciable changes in the shock position (Figs. 4 and 7). For all three porous models, large changes in the pressure distribution occur in the region of porosity and downstream of it. The changes produced are large for the BFH and FFH models.

Fig. 10 Total pressure profiles in the wake,  $M_{S0} = 1.3$ .

A sharp change in the pressure gradient at the beginning of the porous surface can be observed for all three porous models. The shadowgraph for the NH model shows several waves as opposed to one shock wave for the SM. The FFH model shows one primary shock wave followed by a smooth compression. The BFH model shows at least two shock waves.

The pressure distributions corresponding to the position to the shock wave within the porous surface are shown in Fig. 5, and the corresponding shadowgraphs are shown in Fig. 8. The NH model shows upstream influence of holes, with a weak shock wave followed by several waves, the last of which appears to be to the end of the porous surface. The pressure distribution downstream of the porous surface for the NH model shows the possible presence of separation close to the trailing edge of the model. The FFH model shows a trend similar to the NH model in pressure distribution but shows a large variation in pressure when compared with the SM. The BFH model shows the largest change in the pressure distribution downstream of the shock wave, with the shock at the end of the porous region.

The stagnation pressure profiles plotted in the form  $p_0/p_{0\infty}$  vs  $y/c$  for the three shock Mach numbers are shown in Figs. 9-11.

Referring to Fig. 9, the general effect of porosity is to increase viscous losses near the wall and decrease the entropy changes away from the wall, as seen from the changes in the stagnation pressure values across the boundary layer. When compared with the SM model, the NH model shows no appreciable changes. The BFH and FFH models show larger viscous losses but small entropy changes across the shock

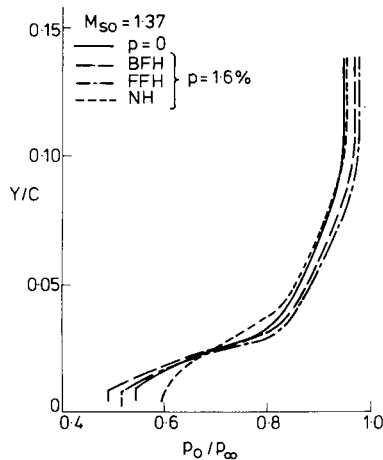


Fig. 11 Total pressure profiles in the wake,  $M_{S0} = 1.37$ .

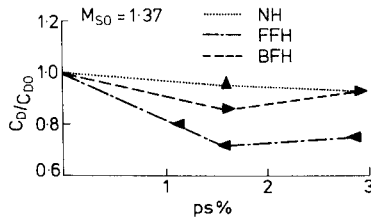


Fig. 12 Variation of drag with shock Mach number.

waves. This trend appears to be true when the shock wave is at the beginning of a porous surface, as seen from Fig. 10. In this case, the BFH produces the largest increase in viscous losses, whereas the FFH produces the smallest entropy changes across the shock waves.

With the shock wave within the porous surface and for the NH model (Fig. 11), there is a small reduction in the viscous losses near the wall, presumably due to the airflow induced by the porous surface, but the reduction in entropy change is not appreciable when compared with the SM. The BFH and FFH models increase the viscous losses near the wall but produce a significant reduction in entropy changes, with the FFH model being the most effective.

The drag coefficients obtained from the investigation of stagnation pressure profiles are plotted in Fig. 12. The values of  $C_D$  for the porous models are normalized with respect to the corresponding values for the SM model for each of the three Mach numbers. The NH model shows a small reduction in drag for  $M_{S0} \geq 1.3$ . At lower Mach numbers, there is actually an increase in drag. Both BFH and FFH show an appreciable reduction in drag for  $M_{S0} < 1.3$ , with the FFH model showing the maximum reduction.

The results of pressure fluctuation measurements for the solid surface and FFH model at two porosities are shown in Figs. 13a and 13b. Figure 13a shows that the effect of porosity is to increase slightly the overall  $\bar{p}/q_{\infty}$  values at lower shock Mach numbers. There is a slight decrease in  $\bar{p}/q_{\infty}$  value at a higher shock Mach number of 1.37 and porosity of 1.07%. Figure 13b shows that the general effect of porosity is to decrease the  $\sqrt{nF(n)}$  at low frequencies typically up to 1 kHz and increase the  $\sqrt{nF(n)}$  values at high frequencies.

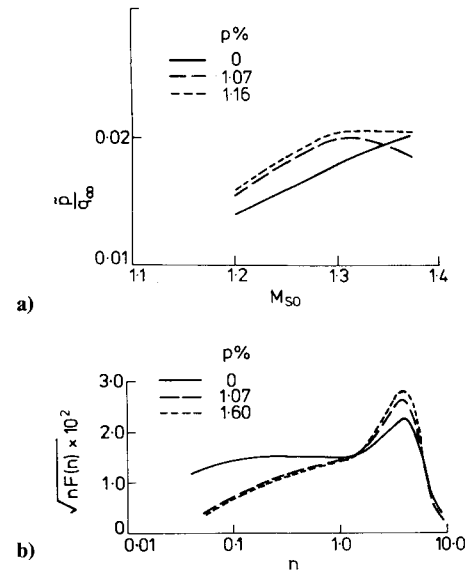


Fig. 13 Effect of porosity on the pressure fluctuations,  $M_{S0} = 1.37$ ,  $X/c = 0.90$ .

## Conclusions

Passive shock-wave/boundary-layer experiments conducted on a roof-mounted 6%-thick part section circular arc model at transonic Mach numbers show that a porous surface made of forward-facing inclined holes produces a larger drag reduction than that produced by normal holes and that passive shock-wave/boundary-layer control can reduce pressure fluctuations in the region of shock/boundary-layer interaction.

## Acknowledgments

This research program is sponsored by the Science and Engineering Research Council. The authors would like to acknowledge the valuable suggestions made by Mr. D. Butter of British Aerospace Group, Manchester.

## References

- <sup>1</sup>Bahi, L., "Passive Shock-Wave/Boundary-Layer Control for Transonic Supercritical Airfoil Drag Reduction," Ph.D. Thesis, Rensselaer Polytechnic Institute, Troy, NY, 1982.
- <sup>2</sup>Bahi, L., Ross, J. M., and Nagamatsu, T., "Passive Shock-Wave/Boundary-Layer Control for Transonic Airfoil Drag Reduction," AIAA Paper 83-0137, Jan. 1983.
- <sup>3</sup>Nagamatsu, H. T., Dyer, R., Troy, N., and Ficarra, R. V., "Supercritical Airfoil Drag Reduction by Passive Shock-Wave/Boundary-Layer Control in the Mach Number Range 0.75 to 0.90," AIAA Paper 85-0207, Jan. 1985.
- <sup>4</sup>Krogman, P. and Stanewsky, E., "Effect of Local Boundary-Layer Suction on Shock Boundary-Layer Interaction and Shock-Induced Separation," AIAA Paper 84-0098, Jan. 1984.
- <sup>5</sup>Savu, G. and Trifu, O., "Porous Airfoils in Transonic Flow," *AIAA Journal*, Vol. 22, July 1984, pp. 989-991.
- <sup>6</sup>Chen, C. L., Chen, Y. C., Holst, T. L., and Van Daisem, W. R., "Numerical Study of Porous Airfoils in Transonic Flow," NASA TM 86713, 1985.
- <sup>7</sup>Mabey, D. G., Welsh, B. L., and Crippos, B. E., "Periodic Flows on a Rigid 14% Thick Biconvex Wing at Transonic Speeds," RAE-TR-810959, 1981.